

Evidence of acid mediated enhancement of photoinduced charge transfer reaction in 2-methoxy-4-(N,N-dimethylamino)benzaldehyde: Spectroscopic and quantum chemical study

Anuva Samanta, Bijan Kumar Paul, Subrata Mahanta, Rupashree Balia Singh, Samiran Kar, Nikhil Guchhait*

Department of Chemistry, University of Calcutta, 92 A.P.C. Road, Kolkata 700009, West Bengal, India

ARTICLE INFO

Article history:

Received 19 January 2010

Received in revised form 30 March 2010

Accepted 19 April 2010

Available online 24 April 2010

Keywords:

2-Methoxy-4-(N,N-dimethylamino)benzaldehyde

Fluorescence

Charge transfer

DFT

TDDFT-PCM

ABSTRACT

The photophysical behavior of 2-methoxy-4-(N,N-dimethylamino)benzaldehyde (2-MDMABA) has been investigated by steady state absorption and emission spectroscopy, time resolved emission spectroscopy and quantum chemical calculations. The molecule 2-MDMABA having a weak acceptor aldehyde group shows strong local emission in all solvents and a weak solvent polarity dependent red shifted emission in polar aprotic solvents for the charge transfer (CT) state which follows well the Lippert–Mataga equation. Instead of usual protonation at the donor site with inhibition of CT process, protonation at the acceptor aldehyde site enhances acceptor properties and hence increases excited state charge transfer reaction. The ground state structural calculation at Density Functional Theory (DFT) level with B3LYP functional and 6-31++ G** basis set and potential energy surfaces (PESs) following twisted intramolecular charge transfer model by using DFT method in the gas phase and in acetonitrile solvent have been performed for the neutral and cation to correlate with experimental findings.

© 2010 Elsevier B.V. All rights reserved.

1. Introduction

Aromatic systems with electron donor and acceptor substituents often exhibit characteristics solvent-dependent spectral properties due to intramolecular charge transfer (ICT) process in the excited states. Molecules possessing an ICT state were used in polymer science in order to get useful insight into the dynamic behavior of the macromolecular media as well as for the study of kinetics of free radical polymerization [1–5]. If the degrees of electron transfer and molecular geometry can be controlled by using the methodology of molecular recognition chemistry, ICT molecules can be used as an excellent tool for detecting ions and molecules and examining microscopic molecular environments.

Since Lippert's first report [6] one of the most extensively studied molecule capable for charge transfer process is the dual fluorescence of 4-(N,N-dimethylamino)benzonitrile (DMABN) [7–14]. Several experimental and theoretical investigations postulate emission from an ICT state twisted about the donor dialkylamino group as well as rotation of the acceptor group [15–26]. Molecules with a flexible single bond between the donor and acceptor sub-

unit are able to rotate around this single bond, thereby stabilizing the ICT state in solvents of large dielectric. According to the twisted intramolecular charge transfer (TICT) hypothesis proposed by Grabowski and co-workers [7,27], 90° internal rotation around a bond connecting a donor group and an acceptor group can decouple the orbital of these two groups and this orbital decoupling provides nearly complete electron transfer from the donor to the acceptor. Consequently, charge separation occurs between the acceptor and the donor, with the acceptor group containing a full negative charge and the donor group containing a full positive charge which results a highly polar twisted excited state. So the ICT molecules show short wavelength emission band for coplanar locally excited state, while the long wavelength band originates from a state with a perpendicular conformation which, under appropriate conditions, can be preferentially stabilized with respect to the planar local excited state. It is found that the emission properties from the charge separated state of the molecule depend on solvent polarity and viscosity [28–30]. Several other hypothesis have been developed in order to explain the unusual emission behavior like solute–solvent exciplex formation [31], planar intramolecular charge transfer (PICT) [32], rehybridized intramolecular charge transfer (RICT) [33,34], wagging intramolecular charge transfer (WICT) [35] and so on. Out of all mechanisms, the TICT model is, nevertheless, the most widely accepted explanation for the dual fluorescence phenomenon of DMABN and other aromatic molecules having donor–acceptor groups [7,15–26].

* Corresponding author. Tel.: +91 33 2350 8386; fax: +91 33 2351 9755.

E-mail addresses: nguchhait@yahoo.com, nikhil.guchhait@rediffmail.com (N. Guchhait).

Molecules exhibiting the presence of an ICT state contain mainly a strong donor dialkylamino group linked by a σ -bond to an aromatic ring having electron-withdrawing residues such as cyano, formyl, carboxyl, ester, sulfonamide groups. Systems with weak charge donor such as primary and secondary amino group and with weak acceptor such as aldehyde group are very uncommon for CT reaction [36]. It is also found that CT reaction is suppressed in presence of acid by preferential binding of H^+ ion at the donor site than at the acceptor site due to more negative charge at the donor site than the acceptor site. In general, DMABN and similar systems show weak LE emission and strong CT emission in highly polar solvents due to facile excited state CT reaction [7,19–26]. On the contrary, it is found that the molecule 4-(N,N-dimethylamino)benzaldehyde (DMABA), a weak acceptor system, shows very weak CT emission [36] and reported spectral data from different groups which are inconsistent [36–41]. Therefore, we have synthesized a substituted DMABA namely 2-methoxy-4-(N,N-dimethylamino)benzaldehyde (2-MDMABA) to throw light on CT reaction of a weakly acceptor system. Purposefully we have tagged –OMe group near the acceptor group to modify the acceptor property and steric effect at the acceptor side. Structurally the presence of –OMe group near the acceptor site increases the electron density at the acceptor site compared to the usual donor site. And thereby insisting the H^+ ion to bind to the acceptor group and consequently increasing the acceptor strength. We have studied the photophysical properties of the neutral molecules in the acidified condition by steady state absorption and emission and time resolved emission spectroscopy. Theoretical studies including solvent effects for the bare molecule and its protonated species have been explored to get a better understanding of the experimental findings. We have performed quantum chemical calculations at DFT level with B3LYP functional and 6-31++G** basis set in the gas phase to find the ground state structural information of the molecule. Considering TICT model the ground and excited state potential energy surfaces for 2-MDMABA and its cation in the gas phase and in acetonitrile solvent have been explored using Density Functional Theory (DFT), Time Dependent Density Functional Theory (TDDFT) and Time Dependent Density Functional Theory–Polarized Continuum Model (TDDFT–PCM) method using same functional and basis set to correlate with experimental results.

2. Experimental

2.1. Materials

The molecule 2-methoxy-4-(N,N-dimethylamino) benzaldehyde was synthesized by the reaction of N,N-dimethyl-m-anisidine with N,N-dimethylformamide and phosphorus oxychloride. Phosphorus oxychloride (1 eqv.) was added slowly in dry DMF at 0 °C and stirred for 30 min. Then N,N-dimethyl-m-anisidine (1 eqv.) in dry DMF was added to the reaction mixture at 0 °C and then slowly warmed to room temperature and stirred for another 2 h. The reaction mixture was poured into ice cold water and neutralized by dropwise addition of aqueous sodium acetate with vigorous stirring and extracted with dichloromethane. The organic layer was washed with water and brine and dried over anhydrous sodium sulfate. The solvent was removed under vacuum to give 2-methoxy-4-(N,N-dimethylamino)benzaldehyde. The compound was purified by column chromatography and repeated crystallization. [1H NMR (300 MHz, $CDCl_3$) δ : 10.14 (s, 1H, CHO), 7.68 (d, J =8.7 Hz, 1H, ArH), 6.26 (d, J =8.7 Hz, 1H, ArH), 6.00 (d, J =2.4 Hz, 1H, ArH), 3.87 (s, 3H, OMe), 3.06 (s, 6H, NMe_2)].

2.2. Solvents

The solvents methylcyclohexane (MCH), acetonitrile (ACN), chloroform ($CHCl_3$), dioxane (DOX), dimethylformamide (DMF),

iso-propanol (i-PrOH), methanol (MeOH) and dimethyl sulfoxide (DMSO) of spectroscopic grade from E-Merck were used as supplied, but only after checking the purity fluorimetrically in the wavelength range of interest. De-ionized water was used for making aqueous solution. Trifluoroacetic acid (TFA) and triethylamine (TEA) from Spectrochem were used as supplied.

2.3. Steady state spectral measurements

The absorption and emission spectra of 2-MDMABA were recorded in different solvents using Hitachi UV/VIS U-3501 spectrophotometer and PerkinElmer (Model LS50B), respectively. For all spectral measurements, the sample concentration was maintained at 10^{-5} to 10^{-6} M in different solvents in order to avoid aggregation and self-quenching.

2.4. Fluorescence lifetime measurements

Fluorescence lifetime measurement has been done by Time Correlated Single Photon Counting (TCSPC) technique using nanoLED-07 (IBH UK) [42]. The light source used in the TCSPC set up is a nanoLED of wavelength 340 nm.

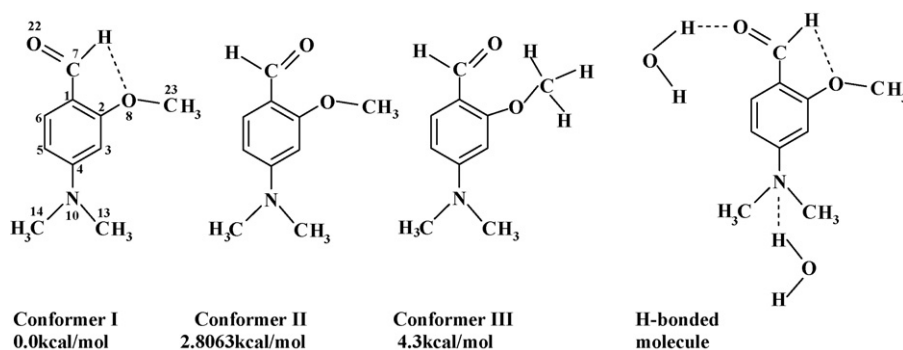
2.5. Computational details

For the structural calculations, the optimized geometry of 2-MDMABA in vacuum at DFT level and in acetonitrile solvent with TDDFT–PCM model, respectively, have been obtained with B3LYP functional and 6-31++G** basis set using Gaussian 03 software [43]. The molecule forms different low energy structures with respect to orientation of flexible substitutions in the ground state [Scheme 1]. The ground and excited state potential energy curves along the donor twist coordinate have been performed by DFT, TDDFT and TDDFT–PCM for gas and solvated phase, respectively, using the same functional and basis set. There are several reported methods for the evaluation of excited properties of donor–acceptor systems [20–26]. The TDDFT method with approximate functional has some restrictions during the evaluation of vertical excitation energies to Rydberg states [44], for the dissociating molecules [45], long range CT excitations for large systems [46], etc. In spite of those limitations, this TDDFT method has been used successfully to ascertain the excited state properties [20–26]. In the ground state, the geometry at different donor twist angles has been kept frozen for the evaluation of PE for the S_0 state. In case of S_1 and S_2 states, vertical transition energies have been calculated with respect to the ground state optimized structure using TDDFT method. For the study of solvent effect on the charge transfer state, the non-relaxed scan has been performed using TDDFT–PCM model. Similar calculations have also been done for the cation too. Though this method of calculation (non-relaxed model) has some restrictions regarding the consideration of frozen geometry, however it has been already used by many scientific groups.

3. Results and discussions

3.1. Absorption spectra

The molecule 2-MDMABA is basically similar to that of DMABA and the $\pi\pi^*$ transition in the absorption spectra is expected to be same in nature. However, this molecule shows two bands in the absorption spectra instead of a single absorption band (\sim 340 nm) for the parent molecule DMABA [36–41]. As seen in Fig. 1a, the observed peaks are at \sim 300 nm (weak) and \sim 340 nm (strong). The $\pi\pi^*$ transition of 2-MDMABA is shifted to the red with respect to benzene due to the presence of substitutions such as $-NMe_2$, $-CHO$ and $-OMe$ groups capable of extra resonance stabilization. As seen in Fig. 1a, the higher energy \sim 300 nm band is practically unchanged



Scheme 1. Different ground state low energy conformers of 2-MDMABA molecule. Calculated energies at DFT (B3LYP/6-31++G**) level are with respect to conformer I.

with the solvent polarity whereas the position of the lower energy peak changes with the dielectric constants and the hydrogen bonding ability of the solvents. The long wavelength absorption band is red shifted with increasing polarity of the solvents and is similar to that of DMABA [36–37]. But the extent of shifting of the absorption peak with solvent polarity is more pronounced in case of DMABA than 2-MDMABA. Comparing the absorption spectra of 2-MDMABA with DMABA and assuming the presence of single species in the ground state, these two peaks are assigned to transition from ground to two excited states. The high absorption intensity for the

low energy band may indicate that this could be a $\pi-\pi^*$ type of transition.

The absorption spectra of 2-MDMABA undergoes a striking change in presence of acid. As seen in the Fig. 1b, gradual addition of strong acid TFA to the acetonitrile solution of 2-MDMABA generates two bands by the expense of the long wavelength absorption band of the neutral species. One of these two bands is red shifted (~ 375 nm) and the other is blue shifted (~ 315 nm) with respect to that of the ~ 340 nm band of the neutral molecule. This may indicate that these two absorption bands may arise due to protonation of the neutral species. Structurally the molecule 2-MDMABA has two protonation sites – one is the nitrogen atom of $-NMe_2$ group and the other is the oxygen atom of $-CHO$ group. Due to the presence of $-OMe$ group at the ortho position of the acceptor group, the charge density at the oxygen atom of $-CHO$ group increases compared to that of the nitrogen atom of $-NMe_2$ group. The $-NMe_2$ group is expected to be coplanar with the aromatic ring in the ground state. Consequently, the lone pair electron of $-NMe_2$ group can delocalize with the π cloud of the aromatic ring. This may decrease the charge density at the $-NMe_2$ group, but increase the same on the oxygen atom of $-CHO$ group. That is why the oxygen atom may prefer protonation first and the large red shifted absorption band could be assigned to the monocation (I) as the generated monocation can be stabilized by resonance (Scheme 2). The addition of another proton to $-NMe_2$ group will shift the spectra to the blue in comparison to that of the neutral molecule. In this case the usual resonance stabilization of the nitrogen lone pair disappears and this observation is common for donor–acceptor systems [20–26].

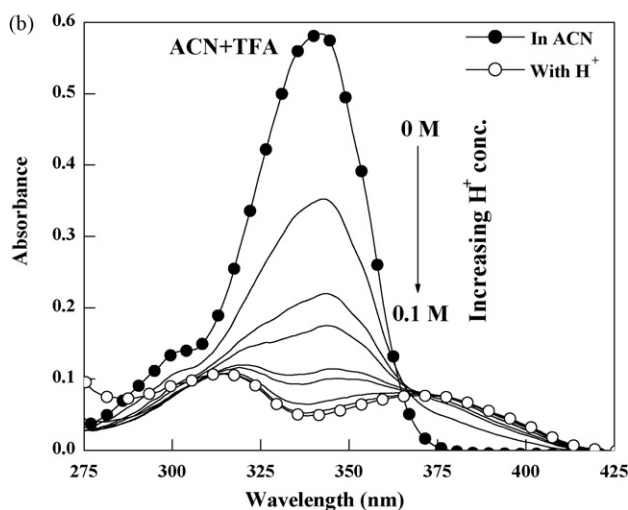
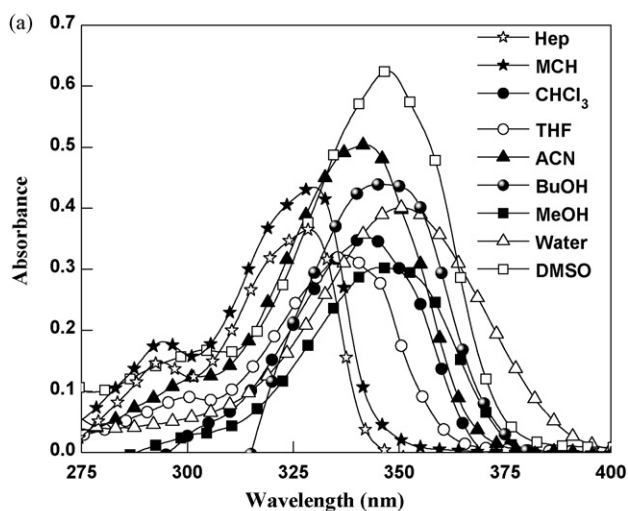
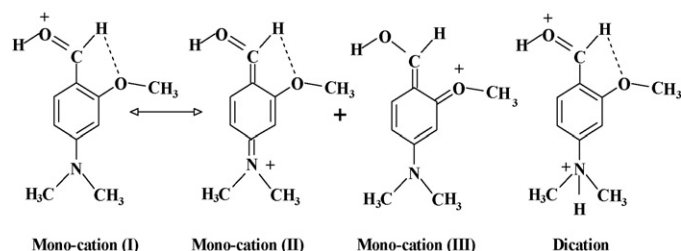


Fig. 1. (a) Absorption spectra of 2-MDMABA in different solvents at room temperature and (b) effect of acid TFA on the absorption spectra of 2-MDMABA in ACN.

3.2. Emission spectra

Room temperature fluorescence emission spectra of 2-MDMABA measured in non-polar, polar and hydrogen bonding solvents are shown in Fig. 2 and the corresponding band maxima are reported in Table 1. In case of non-polar solvents like methyl cyclohexane, on excitation of 2-MDMABA at 330 nm, a single emission at ~ 388 nm is observed with very low fluorescence intensity. It is noteworthy to point out here that DMABA is prac-



Scheme 2. Possible protonated species formed when TFA is added in ACN solution of 2-MDMABA.

Table 1
Spectroscopic parameters obtained from absorption and emission spectra of 2-MDMABA in different solvents at room temperature.

Solvents	λ_{abs} (nm)	λ_{em} (nm)	Stokes' shift ($\Delta\nu$) (cm^{-1})	Quantum yield ^a	
				ϕ_{LE}^f	ϕ_{CT}^f
MCH	330	387	4464	–	–
CHCl ₃	342	384	3164	11.04	–
DCM	343	384	3079	–	–
DOX	343	381	2908	0.16	–
		510	9547		
ACN	341	387	3486	0.62	0.13
		517	9983		
DMF	343	387	3315	1.75	0.45
		521	9961		
i-PrOH	345	380	2670	3.42	–
EtOH	347	383	2709	1.82	–
MeOH	348	390	3094	1.55	–
Water	351	410	4100	0.29	–
DMSO	347	391	3243	0.70	0.09
		529	9915		
Monocation in ACN	375	455	4689	1.16	4.78
		500	6667		
Dication in ACN	315	360	3968	0.50	–

^a Quantum yield $\times 10^{-3}$.

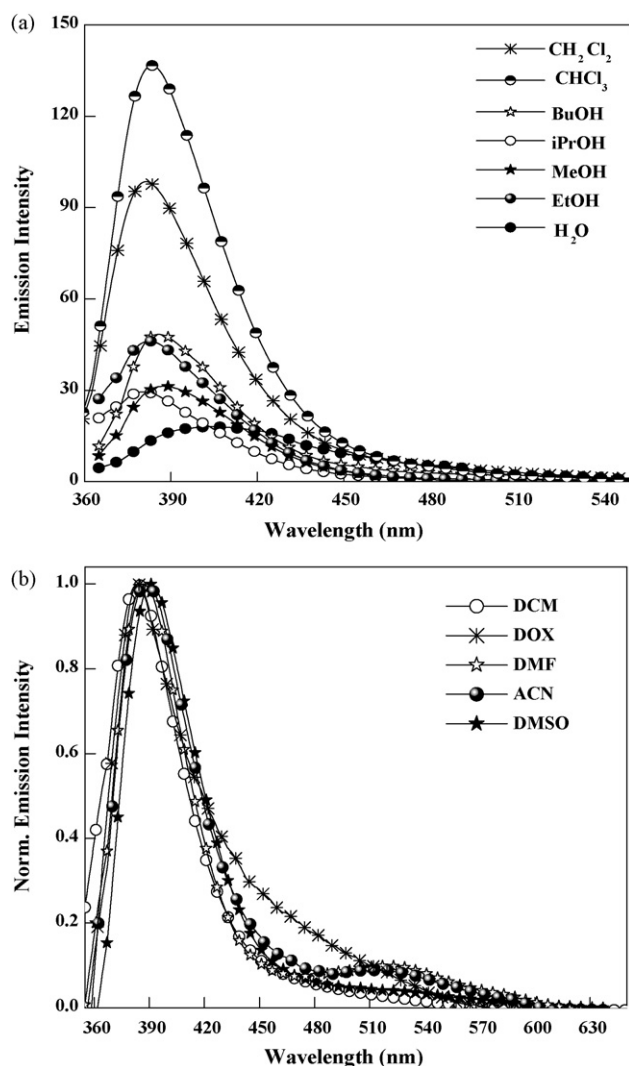


Fig. 2. (a) Fluorescence emission spectra of 2-MDMABA in different solvents at room temperature ($\lambda_{\text{exc}} = 330$ nm for non-polar and $\lambda_{\text{exc}} = 350$ nm for polar protic solvents). (b) Normalized emission spectra of 2-MDMABA in polar aprotic solvents ($\lambda_{\text{exc}} = 340$ nm) at room temperature.

tically non-fluorescent in non-polar solvents. The signature of the spectra predicts that this single emission band is nothing but emission from the LE state of the molecule. Dual emission is observed in polar aprotic solvents upon excitation at 340 nm. The high-energy strong emission band at ~ 385 nm is assigned to LE of the molecule as its position is nearly insensitive to the polarity of the solvents. But the other low energy weakly intense red shifted band at ~ 515 nm shows strong dependency on solvent polarity. Comparing this emissive behavior with DMABA and similar type of systems [15–26], the long wavelength emission band with low intensity is ascribed as charge transfer emission. Due to the presence of the –OMe group, the charge transfer ability as well as solvent dependency of the emission band of 2-MDMABA are further diminished compared to DMABA. The excitation spectra (Fig. 3a) of 2-MDMABA monitored at 385 nm and 515 nm resembles the absorption spectra. Therefore, both the LE and CT bands correspond to the same ground state species which absorbs at ~ 340 nm.

In case of hydroxylic polar solvents, single emission band is observed at ~ 385 nm. In addition to the decrease in energy of the CT state by dielectric stabilization, the intermolecular hydrogen bonding interaction with protic solvents opens up usual non-radiative channels. That may be the reason of observing only LE emission in protic solvents. The absence of CT emission of DMABA in protic solvents was explained by considering stabilization of the CT state [47]. It is proposed that the stabilization of the CT state reduces the energy gap between the ICT state and the Franck–Condon state resulting in a rapid non-radiative decay of the ICT state to the low-lying state [47]. In ACN, 2-MDMABA shows two emission bands corresponding to LE and CT state of the molecule. When methanol was added to that solution, a decrease of intensities of both the bands is noticed (Fig. 3b). This result is consistent with the facts that increase in polarity and H-bonding parameter increases the non-radiative rate and thus decreases the fluorescence intensity of both the bands.

The effect of the nature of the solvent on the energy difference between the ground and excited states of a molecule depends on the refractive index (n) and dielectric constant (ϵ_r) of the solvent and is described by the following Lippert–Mataga equation [48].

$$\Delta\nu = \nu_a - \nu_f = \frac{(\mu^* - \mu)^2}{2\pi\epsilon_0\hbar c\rho^3} f(\epsilon_r, n)$$

where $f(\epsilon_r, n) = [(\epsilon_r - 1)/(2\epsilon_r + 1)] - [(n^2 - 1)/(2n^2 + 1)]$.

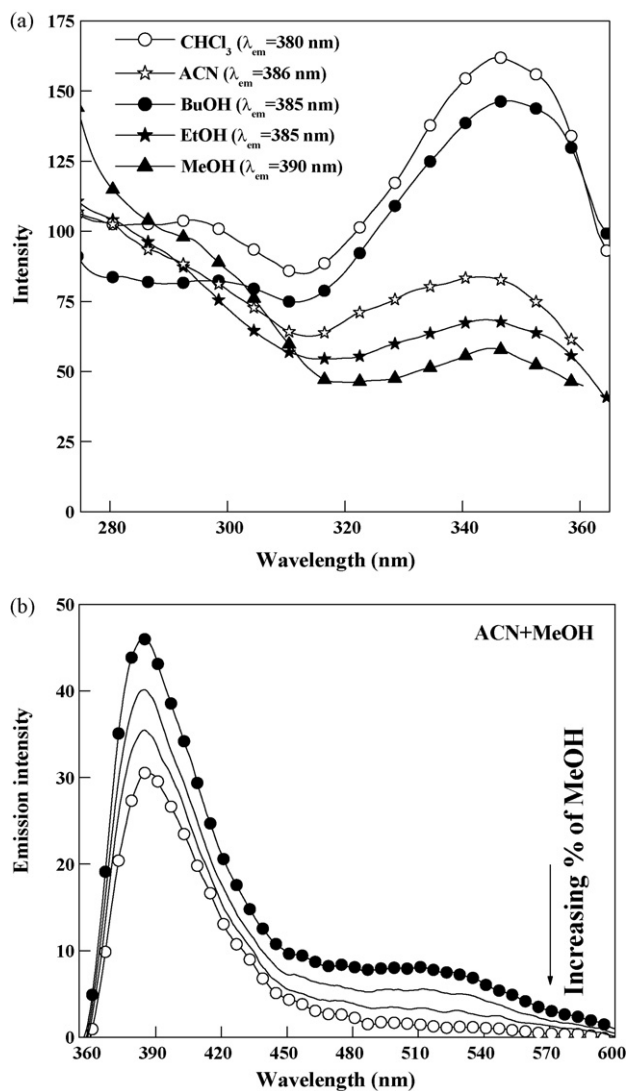


Fig. 3. (a) Excitation spectra of 2-MDMABA in different solvents at room temperature. (b) Effect of mixed solvent (ACN+MeOH) on the emission spectra ($\lambda_{\text{ext}} = 340$ nm) of 2-MDMABA.

In this equation, ν_a and ν_f are the wavenumber (cm^{-1}) of absorption and emission band maxima, respectively. The symbol ϵ_0 , h , c are permittivity of vacuum ($8.85 \times 10^{-12} \text{ V C}^{-1} \text{ m}^{-1}$), Planck's constant ($6.626 \times 10^{-34} \text{ J s}$) and velocity of light ($3 \times 10^8 \text{ m s}^{-1}$), respectively. The radius of cavity (ρ) in which the fluorophore resides and the ground state dipole moment (μ) have been computed for the global minimum structure of 2-MDMABA calculated at DFT level using B3LYP functional and 6-31++G** basis set and the corresponding values are 4.74 and 7.98 Debye (The values for DMABA are 4.3 Å and 5.6 D, respectively, at the same level of calculation.) [36]. The excited state dipole moment can be obtained from the slope of the plot of Stokes shift ($\Delta\nu$) versus solvent polarity parameter (Δf) (Fig. 4). Though the changes in absorption and emission peak with solvent dielectric are not so pronounced, but their differences i.e., $\Delta\nu$ changes linearly with Δf values. The calculated dipole moment of the excited state from the solvatochromic measurement is found to be 12.03 D ($\mu_e^{\text{CT}} = 12 \text{ D}$ for DMABA) [36]. Therefore, high dipole moment due to atomic charge redistribution in the excited state by charge transfer from -NMe₂ group to -CHO group is responsible for the polarity dependent Stokes shifted emission.

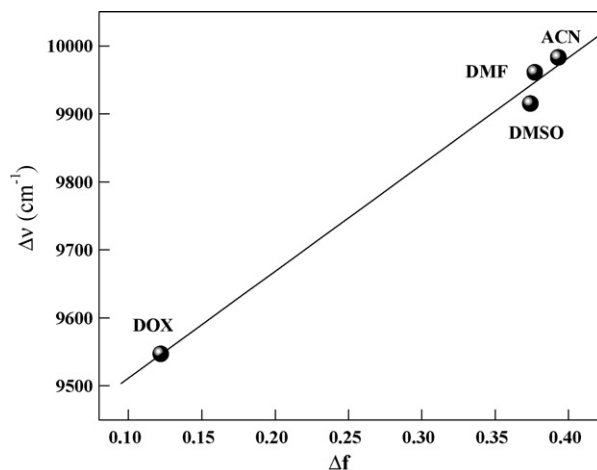


Fig. 4. (a) Plot of Stokes shift ($\Delta\nu$) versus solvent parameter (Δf).

In 2-MDMABA, due to the presence of -OMe group, the aldehyde group is expected to be more basic than the tertiary amino group and it is opposite to that of DMABA. Hence oxygen atom of -CHO is expected to be protonated first before protonation at the nitrogen lone pair of N,N-dimethylaniline group. As seen in the Fig. 5a, after addition of TFA to the ACN solution of 2-MDMABA both the LE and CT band disappear and a new broad band peaks at 500 nm. As discussed earlier in Section 3.1, strong acid TFA may insist protonation at both the centers with the formation of both monocation and dication. The electron-pulling ability of the acceptor must increase after first protonation at the aldehyde oxygen atom and the generated monocation is expected to show a large red shift emission band for a favorable charge transfer emission from the monocationic species. Second protonation, i.e., protonation at the nitrogen centre insists the absence of CT emission due to unavailability of the nitrogen lone pair. When the protonated species (dication) is excited at 315 nm, two emission bands are observed – one at ~ 360 nm and broad band ~ 480 nm (Fig. 5b). As seen in Fig. 6a, the excitation spectra monitored at 360 nm and 480 nm resemble with the absorption spectra of dication and monocation, respectively. Therefore, the emission band at 360 nm is assigned to the local emission of doubly protonated species whereas the broad emission band may arise from the monocation form generated from the dication in the excited state surface after deprotonation. Interestingly, a broad emission band of the monocation appears at ~ 455 nm on excitation at 375 nm. As shown in inset of Fig. 5b, this broad emission band after deconvolution using Gaussian fit shows two bands – one at ~ 450 nm and another at ~ 500 nm. As the excitation spectra monitored at 450 and 500 nm are same, the low energy red shifted emission band at 500 nm band is assigned to the charge transfer emission of the monocation arising from the deprotonation of the dication. The electron-pulling ability of the monocation is more than the neutral molecule, that is why the charge transfer intensity of the protonated species is very high. The relationship between the neutral (N), monoprotonated (M) and doubly protonated (D) forms is summarized in Scheme 3. When methanol is added, the rate of deprotonation decreases, as a result of which the intensity of the CT band of monocation is diminished (Fig. 6b). In a protic solvent or an aprotic solvent mixed with a protic solvent, the excited state deprotonation process does not occur. The excitation spectra monitored at 400 nm in the presence of methanol is same as that of the dication. In the presence of protic solvent, only dication is present.

The fluorescence quantum yields are measured relative to β -naphthol in MCH. As shown in Table 1, it is found that the fluorescence quantum yield for the CT emission of 2-MDMABA in different solvents is lower than the LE emission band. This may indicate that

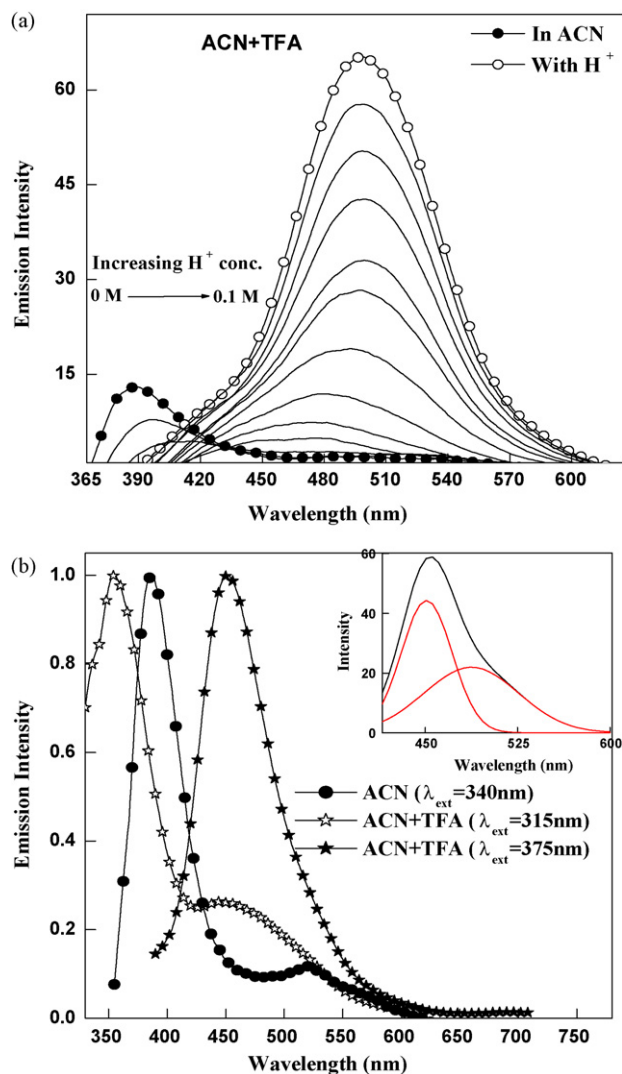


Fig. 5. (a) Effect of TFA on the emission spectra of 2-MDMABA in ACN ($\lambda_{\text{ext}} = 340$ nm) and (b) normalized emission spectra of monocation and dication of 2-MDMABA (Inset: deconvoluted figure of the protonated form of 2-MDMABA using Gaussian fit).

LE to CT conversion is less favorable. It is worthwhile to note that the fluorescence quantum yield for the CT band of DMABA is higher than 2-MDMABA [37,41]. This is in accord with the expectation for 2-MDMABA with a slightly lower electron affinity of the acceptor due to the ortho substitution. The fluorescence quantum yield in polar protic solvents is low due to activation of non-radiative channels by intermolecular H-bonding interaction.

The fluorescence lifetime of 2-MDMABA in acetonitrile solvent shows that the fluorescence decay of LE band (390 nm) is 0.0581 ns ($\chi^2 = 1.0963$) and that of the CT band (510 nm) is 0.6179 ns ($\chi^2 = 1.1.1032$) whereas mean fluorescence lifetime of DMABA ranges from 0.45 to 1.74 ns [36]. On the other hand in protic solvent water, the LE emission shows single exponential decay with decay time 0.028 ns ($\chi^2 = 1.1032$). The decrease in fluorescence lifetime in hydrogen bonding solvent may be due to channel out of energy by hydrogen bonding interaction [49].

3.3. Quantum chemical calculation

The ground state structure of 2-MDMABA and potential energy surfaces along the CT reaction path have been calculated at DFT level with Becke's three parameter hybrid functional (B3LYP) and

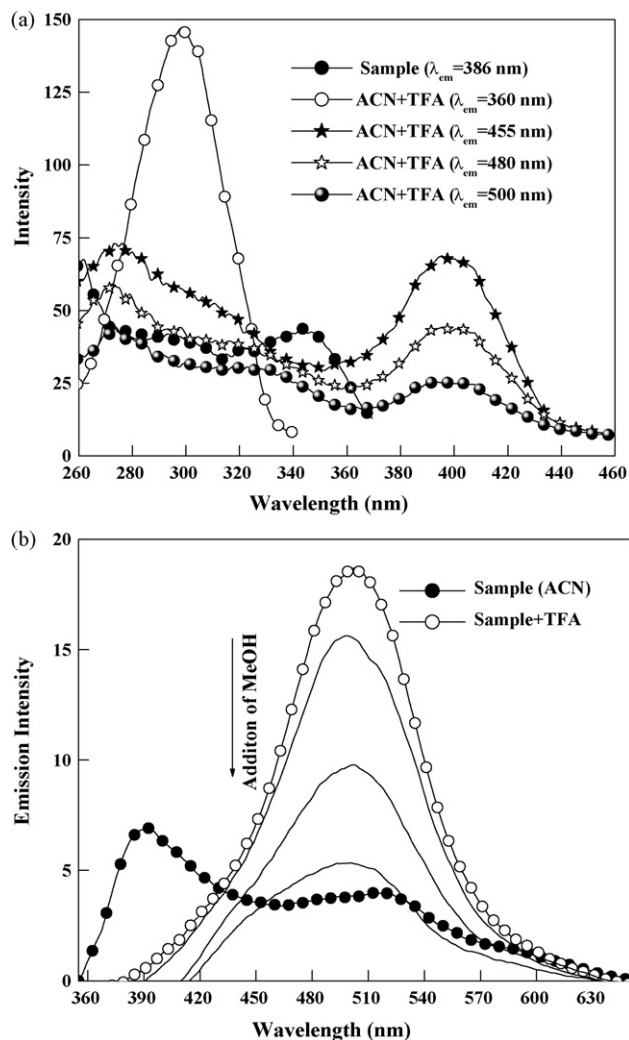
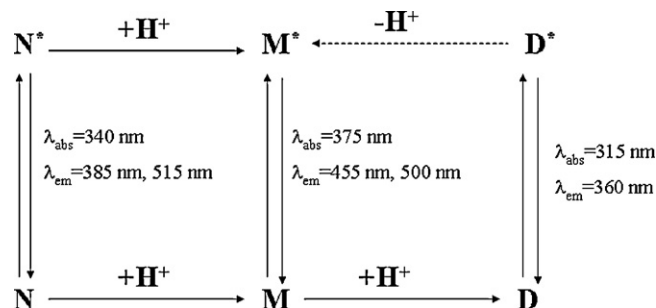


Fig. 6. (a) Excitation spectra of protonated species monitored at different emission wavelength and (b) effect of addition of methanol on the emission spectra of protonated species of 2-MDMABA.

6-31++G** basis set to correlate the observed excited state phenomenon of the studied molecule. In the ground state the molecule 2-MDMABA shows three low energy conformers. Among these three conformers, conformer I (Scheme 1) is found to be the most stable structure due to stabilization by intramolecular H-bonding. Two other structures are quite high-energy conformers due to the possible steric interaction of the neighboring -OMe substitution. The selective optimized parameters for the lowest energy conformer are presented in Table 2. It is to note that the global



Scheme 3. The relationship between the neutral (N), the monocation (M) and the dication (D) of 2-MDMABA in the ground state as well as excited state.

Table 2

Structural parameters for the optimized ground state lowest energy conformer of 2-MDMABA at DFT level with B3LYP functional and 6-31++G** basis set.

Bond	Calculated values (Å)	Angle/dihedral angle	Calculated values (°)
R _{C1-C2}	1.417	<C13–N10–C14	119.390
R _{C2-C3}	1.395	<C13–N10–C4	120.148
R _{C3-C4}	1.418	<C1–C7–O22	124.069
R _{C6-C1}	1.405	<C1–C2–O8	116.142
R _{C1-C7}	1.467	<C3–C4–N10–C13	0.013
R _{C7-O22}	1.228		
R _{C2-O8}	1.365		
R _{O8-C23}	1.422		
R _{C4-N10}	1.377		
R _{N10-C13}	1.454		
R _{N10-C14}	1.457		

minimum structure (Conformer I) of 2-MDMABA has a nearly planar geometry at the nitrogen centre where –NMe₂ group is in the plane of the benzene ring (<C3–C4–N10–C13 = 0.013). So, there is a possibility of extensively delocalized of the lone pair of nitrogen atom to the benzene π -ring in the ground state. Hence the calculated Mulliken charges over the nitrogen atom (–0.062) of –NMe₂ is quite lower than the oxygen atom (–0.420) of –CHO group. In case DMABA, the Mulliken charges over nitrogen and oxygen atoms are –0.510 and –0.441, respectively at the same level of calculation [50]. Extensive delocalization of nitrogen lone pair electron for 2-MDMABA reduce electron charge at nitrogen atom and the presence of –OMe group enhances the electron density over the oxygen atom of –CHO group. This may be the reason why first protonation occurs at the oxygen atom of aldehyde group instead of usual protonation at the donor site like DMABA.

Fig. 7 shows the angular dependency of energy for the ground and first excited state by rotational motion of the donor group around the benzene plane in vacuum using DFT and TDDFT method and in acetonitrile solvent using TDDFT–PCM model. The ground state potential energy surface shows an increase in energy upon rotation of the dimethylamino group. In vacuum and in ACN solvent, an energy-stabilized twisted geometry ($\theta = 90^\circ$) is found in the S₁ surface. In the S₁ PES, the transition from planar to twisted state occurs through a barrier and the height of the barrier in vacuum is higher than in ACN solvent. The occurrence of TICT implies the existence of two close lying energy states i.e., the LE and CT states. The first emission takes place from the LE state and the low energy emission occurs from the CT state after relaxation to a perpendicular structure from the LE state through a barrier. The energy barrier for the transformation from LE to CT state is 5.76 kcal/mol in vacuum and 2.64 kcal/mol in ACN solvent. This barrier may arise from the decrease of delocalization of nitrogen lone pair along the twist coordinate compared to the planar conformation of 2-MDMABA in the global minimum state with maximum delocalization of lone pair of nitrogen atom with aromatic moiety. The low barrier energy in ACN indicates the feasibility of CT in the excited state in polar solvent. Comparing the calculated barrier energy of 2-MDMABA (5.76 and 2.64 kcal/mol in vacuum and in ACN, respectively) with DMABA (4.64 and 0.38 kcal/mol in vacuum and in ACN, respectively) [50], it is obvious that LE to CT transition is more feasible for DMABA due to very low crossover energy than 2-MDMABA. The experimentally and theoretically values of vertical transition energies in vacuum and in ACN are presented in Table 3. It is clearly found that the theoretical values are in well agreement with the respective experimental values. Theoretically it is expected that $\pi\pi^*$ transition having high oscillator strength value is allowed transition and $n\pi^*$ transition is forbidden transition having low oscillator strength value. It is clear from the plot of oscillator strength versus twist angle (Fig. 8) that LE emission is of $\pi\pi^*$ type ($f = 0.1803$) and CT emission is $n\pi^*$ type ($f = 0.0079$). As the CT state has low oscillator

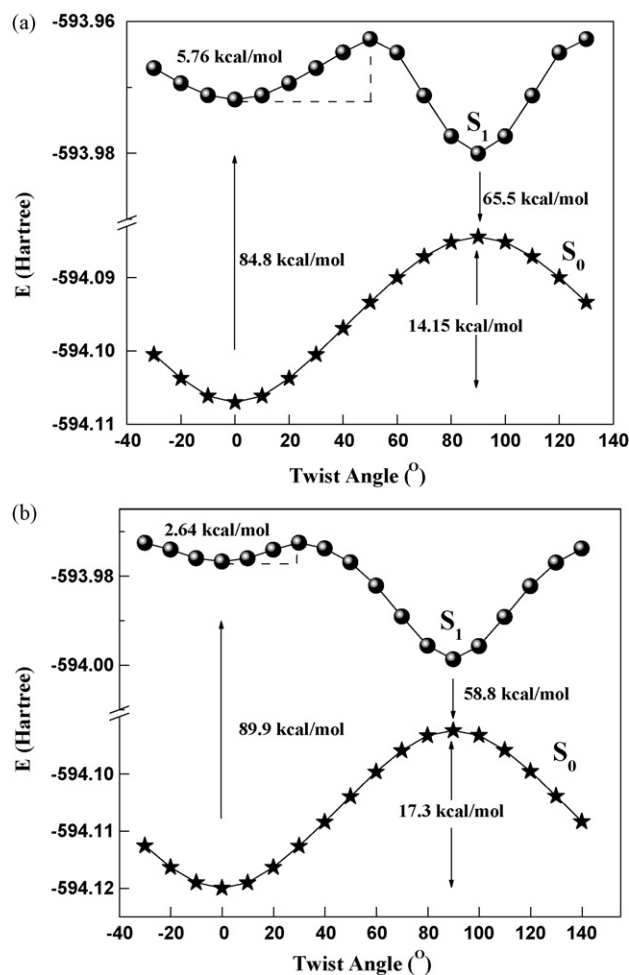


Fig. 7. Potential energy curves of 2-MDMABA for the S₀ and S₁ states along the donor twisting coordinate in (a) vacuum and (b) ACN solvent using DFT (B3LYP/6-31++G**) level (TDDFT for S₁ state and TDDFT–PCM for ACN solvent).

strength value, the emission intensity of the CT state is low compare to the LE state. From the HOMO–LUMO picture (Fig. 9), it is seen that the π cloud density is delocalized over the entire aromatic ring for the HOMO (π) and LUMO (π^*) due to planar configuration of the global minimum structure. So $\pi\pi^*$ transition occurs for non-twisted geometry. During the twisting of the donor group ($\theta = 90^\circ$), the lone pair is localized over the nitrogen atom for HOMO (n) and LUMO is of π^* character. In the CT state, HOMO–LUMO transition is $n\pi^*$ type having very low oscillator strength value. Very similar trend is observed in ACN solvent where calculated oscillator strength decreases from 0.5038 for the global minimum

Table 3

Comparison between experimental and computed energy (eV) for different excited states of 2-MDMABA and the monocation in vacuum and acetonitrile at DFT level with B3LYP functional and 6-31++G** basis set.

Medium/solvent	Absorption			Emission		
	State	E_{th}	E_{ex}	State	E_{th}^a	E_{ex}^a
Vacuo	S ₁	3.66	3.75	S ₁	2.83	3.20
	S ₂	4.09	4.20	S ₂	–	–
ACN	S ₁	3.88	3.64	S ₁	2.54	2.39
	S ₂	3.99	4.11	S ₂	–	–
Cation in ACN	S ₁	3.55	3.35	S ₁	1.29	2.48

^a Emission from CT state. E_{th} and E_{ex} are theoretical and experimental energies, respectively.

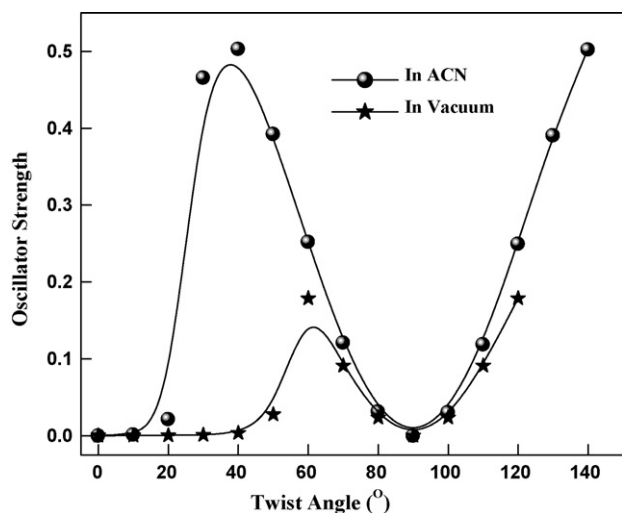
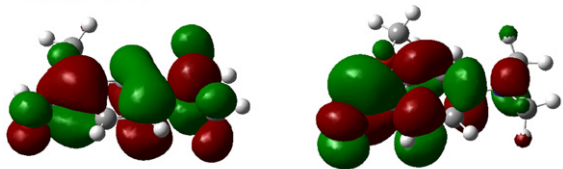


Fig. 8. The variation of oscillator strength of 2-MDMABA with varying donor twist angle in (a) vacuum and (b) ACN solvent.

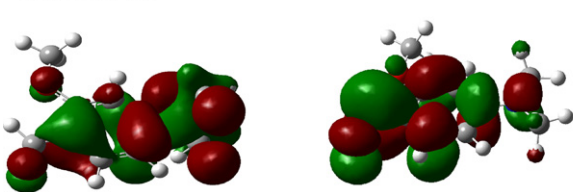
structure to 0.0083 in the twisted form. The HOMO–LUMO picture supports that localization of electron density over nitrogen atom in the twisted form favors the CT process.

We have also performed potential energy surface calculation for the monocationic species using the same method as is done for the neutral molecule. The ground state behavior of the cation is quite same as that of the neutral molecule. The barrier to the conversion from LE to CT along the donor coordinate in the first excited state is found to be 4.02 kcal/mol (Fig. 10a) and it is lower than the neutral molecule (5.76 kcal/mol). On the other hand, while we consider the solvent effect on the monocation, it is noticed that the barrier energy for the first excited state (Fig. 10b) of the monocation is quite

A. Vacuum ($\theta=0^\circ$)



B. Vacuum ($\theta=90^\circ$)



C. ACN ($\theta=90^\circ$)

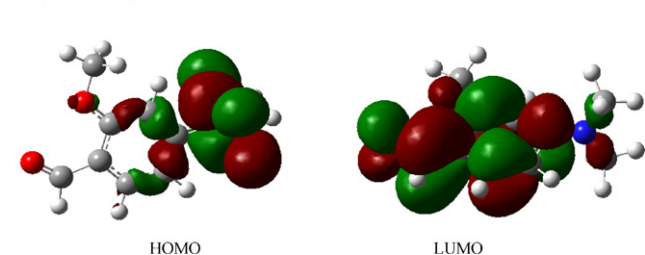


Fig. 9. HOMO and LUMO picture of 2-MDMABA in (a) vacuum ($\theta=0^\circ$), (b) vacuum ($\theta=90^\circ$), and (c) ACN ($\theta=90^\circ$) solvent obtained from calculated structure at DFT level.

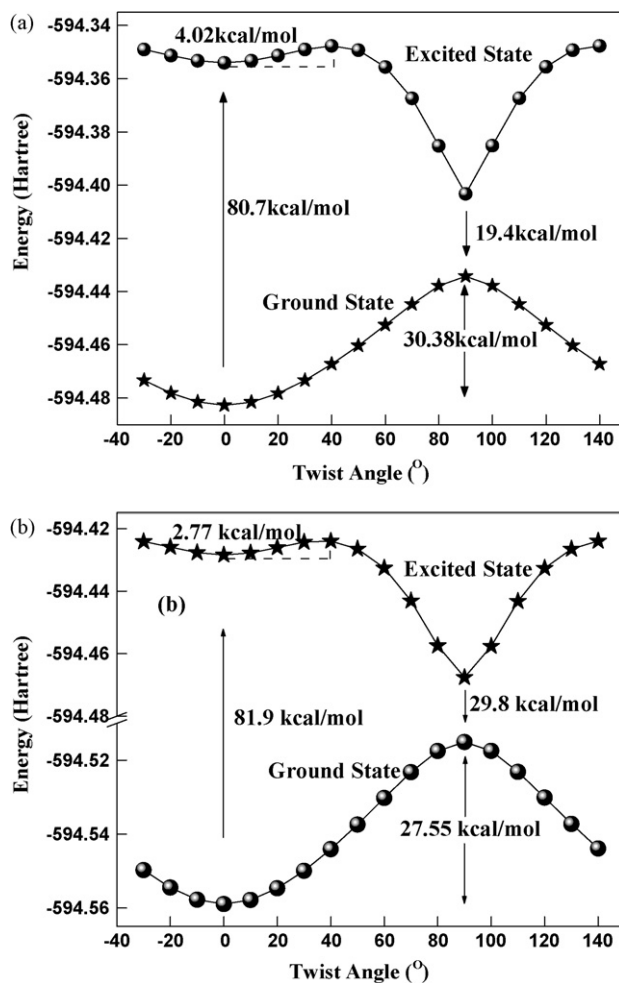


Fig. 10. Potential energy curves of the monocation of 2-MDMABA for the S_0 and S_1 states along the donor twisting coordinate in (a) vacuum and (b) ACN solvent using DFT (B3LYP/6-31++G**) method (TDDFT for S_1 state and TDDFT-PCM for ACN solvent).

same as neutral molecule (2.77 and 2.64 kcal/mol for monocation and neutral molecule, respectively). It is seen from Figs. 7 and 10 that the calculated vertical transition energy for the cation is low than the corresponding neutral species and this is in right trend with the experimental observation. As seen in Fig. 10, the calculated electronic excitation energy for the crossing from LE to CT transition is ~ 84.7 kcal/mol for the cation both in vacuum and in ACN solvent which can be accessible upon photoexcitation at ~ 340 nm (~ 84.1 kcal/mol). But in case of neutral molecule, the same calculated electronic excitation energy for the conversion from LE to CT is ~ 90 – 92 kcal/mol which is not easily accessible by ~ 340 nm excitation. This also supports a favorable photoinduced charge transfer reaction for the monocation than the neutral molecule. Calculated oscillator strength for the monocation is found to be similar to that of the neutral species where local excitation is of $\pi\pi^*$ type with high oscillator strength having the planar geometry and charge transfer emission is of $n-\pi^*$ type with low oscillator strength having 90° twisted geometry.

4. Conclusion

In this paper, donor–acceptor substituted aromatic system namely 2-methoxy-4-(N,N-dimethylamino)benzaldehyde having a weak acceptor group has been synthesized and the excited state properties of its neutral, monocation and dication have been inves-

tigated by steady state and time resolved spectral measurement. In addition to the local emission the molecule shows weak charge transfer emission in polar aprotic solvents. The molecule favors CT emission in presence of acid due to enhancement of acceptor strength by protonation at the acceptor site instead usual protonation at the donor site. The substituted methoxy group is responsible for such acid induced enhancement of CT emission. Excited state deprotonation of the dication produces CT emission from the monocation. Mulliken charge distribution at the donor and acceptor sites for the calculated structure of neutral and monocation at DFT (B3LYP/6-31++G**) level well predicts the enhancement of acceptor strength by acidification. Theoretical PESs for the ground and excited state along the donor twist coordinate using TICT model for the neutral and monocation in the vacuum and ACN solvent clearly predict the red shifted CT emission in the S_1 surface at 90° twisted geometry. The lowering of LE to CT barrier energy from vacuum to ACN solvent and also from neutral to monocation well correlates the experimental spectral observations.

Acknowledgements

NG acknowledges CSIR, India (Project no. 01(2161)07/EMR-II) and DST, India (Project No. SR/S1/PC/26/2008) for financial support. The authors would like to thank Prof. T. Ganguly of IACS, Kolkata for allowing them fluorescence lifetime measurements. AS and BKP thank CSIR for Junior Research Fellowship.

References

- [1] R. Hayashi, S. Tuzuke, C.W. Frank, *Macromolecules* 20 (1987) 983–988.
- [2] S. Tuzuke, R. Kun Guo, R. Hayashi, *Macromolecules* 21 (1988) 1046–1051.
- [3] S. Tuzuke, R. Kun Guo, R. Hayashi, *Macromolecules* 22 (1989) 729–734.
- [4] A. Bajorek, J. Paczkowski, *Macromolecules* 31 (1998) 86–95.
- [5] J. Paczkowski, D.C. Neckers, *Macromolecules* 24 (1991) 3013–3016.
- [6] E. Lippert, W. Luder, H. Boos, *Advances in Molecular Spectroscopy*, Pergamon Press, Oxford, 1962, pp. 443–457.
- [7] K. Rotkiewicz, K.H. Grellman, Z.R. Grabowski, *Chem. Phys. Lett.* 19 (1973) 315–318.
- [8] E.M. Kosower, H. Dodiuk, *J. Am. Chem. Soc.* 98 (1976) 924–929.
- [9] D. Majumder, R. Sen, K. Bhattacharyya, S.P. Bhattacharyya, *J. Phys. Chem.* 95 (1991) 4324–4329.
- [10] G.K. Schenter, C.B. Duke, *Chem. Phys. Lett.* 176 (1991) 563–570.
- [11] S. Marguet, J.C. Mialocq, P. Millie, *Chem. Phys.* 160 (1989) 265–279.
- [12] J.P. LaFemina, C.B. Duke, A. Patton, *J. Chem. Phys.* 87 (1987) 2151–2157.
- [13] S. Hayashi, K. Ando, S. Kato, *J. Phys. Chem.* 99 (1995) 955–964.
- [14] A. Gorse, M. Pesquer, *J. Phys. Chem.* 99 (1995) 4039–4049.
- [15] Z. Grabowski, K. Rotkiewicz, W. Rettig, *Chem. Rev.* 103 (2003) 3899–4032.
- [16] D. Rappoport, F. Furche, *J. Am. Chem. Soc.* 126 (2004) 1277–1284.
- [17] A. Kohn, C. Hattig, *J. Am. Chem. Soc.* 126 (2004) 7399–7410.
- [18] A. Parusel, *J. Chem. Soc., Faraday Trans.* 94 (1998) 2923–2928.
- [19] P.R. Bangal, S. Panja, S. Chakravorty, *J. Photochem. Photobiol. A: Chem.* 139 (2001) 5–16.
- [20] A. Chakraborty, S. Kar, N. Guchhait, *J. Phys. Chem. A* 110 (2006) 12089–12095.
- [21] A. Chakraborty, S. Kar, N. Guchhait, *J. Photochem. Photobiol. A: Chem.* 181 (2006) 246–256.
- [22] A. Chakraborty, S. Kar, N. Guchhait, *Chem. Phys.* 324 (2006) 733–741.
- [23] A. Chakraborty, S. Kar, N. Guchhait, *Chem. Phys.* 320 (2006) 75–83.
- [24] S. Mahanta, R.B. Singh, S. Kar, N. Guchhait, *J. Photochem. Photobiol. A: Chem.* 194 (2008) 318–326.
- [25] R.B. Singh, S. Mahanta, S. Kar, N. Guchhait, *Chem. Phys.* 342 (2007) 33–42.
- [26] R.B. Singh, S. Mahanta, S. Kar, N. Guchhait, *J. Lumin.* 128 (2008) 1421–1430.
- [27] Z. Grabowski, K. Rotkiewicz, A. Siemiarczuk, D. Cowley, W. Baumann, *Nouv. J. Chim.* 3 (1979) 443–454.
- [28] W. Rettig, *J. Lumin.* 26 (1980) 21–46.
- [29] W. Rettig, *J. Phys. Chem.* 86 (1982) 1970–1976.
- [30] R. Hayashi, S. Tuzuke, C.W. Frank, *Chem. Phys. Lett.* 135 (1987) 123–127.
- [31] E.A. Chandross, in: Gordon, Ware (Eds.), *The Exciplex*, Academic Press, New York, 1975, pp. 187–207.
- [32] Y.V. Ilichev, W. Kühnle, K.A. Zachariasse, *J. Phys. Chem. A* 102 (1998) 5670–5680.
- [33] A. Sobelowski, W. Sudholt, W. Domcke, *J. Phys. Chem. A* 102 (1998) 2716–2722.
- [34] K.W. Zachariasse, T. von der Haar, A. Hebecker, U. Leinhos, W. Kühnle, *Pure Appl. Chem.* 65 (1993) 1745–1750.
- [35] B. Mennucci, A. Toniolo, J. Tomasi, *J. Am. Chem. Soc.* 122 (2000) 10621–10630.
- [36] A. Kowski, B. Kukliński, P. Bojarski, *Chem. Phys. Lett.* 448 (2007) 208–212.
- [37] N. Chottopadhyay, J. Rommens, M.V. Auweraer, F.C.D. Schryver, *Chem. Phys. Lett.* 264 (1997) 265–272.
- [38] J. Dobkowski, E. Kirkor-Kamińska, J. Koput, A. Siemiarczuk, *J. Lumin.* 27 (1982) 339–355.
- [39] S. Dähne, W. Freyer, K. Teuchner, J. Dobkowski, Z.R. Grabowski, *J. Lumin.* 22 (1980) 37–49.
- [40] Z.R. Grabowski, J. Dobkowski, *Pure Appl. Chem.* 55 (1983) 245–252.
- [41] Z.R. Grabowski, J. Dobkowski, W. Kühnle, *J. Mol. Struct.* 114 (1984) 93–100.
- [42] P. Mandal, S. Kundu, T. Misra, S.K. Roy, T. Ganguly, *J. Phys. Chem. A* 111 (2007) 11480–11486.
- [43] M.J. Frisch, et al., *Gaussian 03, Revision B.03*, Gaussian, Inc., Pittsburgh, PA, 2003.
- [44] C. Adamo, G.E. Scuseria, V. Barone, *J. Chem. Phys.* 111 (1999) 2889–2899.
- [45] Z.L. Cai, J.R. Reimers, *J. Chem. Phys.* 112 (2000) 527–530.
- [46] J. Neugebauer, O. Gritsebko, E. Jan Baerends, *J. Chem. Phys.* 124 (2006) 214102.
- [47] S. Kundu, N. Chattopadhyay, *J. Mol. Struct.* 344 (1995) 151–155.
- [48] N. Mataga, H. Chosrowjan, S. Taniguchi, *J. Photochem. Photobiol. C: Photochem. Rev.* 6 (2005) 37–79.
- [49] A. Cser, K. Nagy, L. Biczók, *Chem. Phys. Lett.* 360 (2002) 473–478.
- [50] A. Samanta, B.K. Paul, N. Guchhait, in press.